processes

MDPI

Article

Exploring Principal Component Analysis for Enhanced Insights into Physical and Operational Characteristics of Palladium-Based Membrane Composites: Advancing Hydrogen (H_2) Energy Potential to Revolutionize the Energy Sector

Khaled Younes [1,*], Walid Al-Shaar [1], Majdi Hochlaf [2], Maroua Fattouche [3], Salah Belaidi [3] and Christina El Sawda [1]

[1] College of Engineering and Technology, American University of the Middle East, Egaila 54200, Kuwait; walid.alshaar@aum.edu.kw (W.A.-S.); christina.el-sawda@aum.edu.kw (C.E.S.)
[2] COSYS/IMSE, Université Gustave Eiffel, 5 Boulevard Descartes Champs-sur-Marne, 77454 Marne-la-Vallée, France; majdi.hochlaf@univ-eiffel.fr
[3] Group of Computational and Medicinal Chemistry, Molecular Chemistry and Environment Laboratory, University of Biskra, BP 145, Biskra 07000, Algeria; maroua.fattouche@univ-biskra.dz (M.F.); s.belaidi@univ-biskra.dz (S.B.)
* Correspondence: khaled.younes@aum.edu.kw

Abstract: In this study, we used Principal Component Analysis (PCA) to evaluate the physical and operational properties of palladium (Pd)-based membrane composites, focusing on variables like temperature, differential pressure (ΔP), thickness, hydrogen (H_2) permeability, and H_2 flux. The analysis revealed that the first two principal components explained 53.16% of the total variance, indicating moderate explanatory power. Interdependencies were observed among temperature, thickness, H_2 flux, and H_2 permeability, while ΔP functioned independently. This study found similarities among membranes, such as eco-friendly chitosan-based membranes, which performed comparably to conventional options like Pd–PSS and Pd–Cu/αAl_2O_3. Overall, PCA proved to be an invaluable tool for uncovering hidden patterns, optimizing experimental processes, and deepening the understanding of Pd-based membranes. The findings underscore PCA's potential to enhance material performance and promote sustainable alternatives, with practical benefits for advancing hydrogen separation technologies. This study illustrates how data-driven approaches can refine material analysis and drive innovation in membrane design.

Keywords: operational conditions; principal component analysis; hydrogen production; palladium-based membrane composites; energy sector

check for updates

Academic Editors: Sake Wang, Nguyen Tuan Hung and Minglei Sun

Received: 11 December 2024
Revised: 6 January 2025
Accepted: 8 January 2025
Published: 11 January 2025

Citation: Younes, K.; Al-Shaar, W.; Hochlaf, M.; Fattouche, M.; Belaidi, S.; El Sawda, C. Exploring Principal Component Analysis for Enhanced Insights into Physical and Operational Characteristics of Palladium-Based Membrane Composites: Advancing Hydrogen (H_2) Energy Potential to Revolutionize the Energy Sector. *Processes* **2025**, *13*, 192. https://doi.org/10.3390/pr13010192

Copyright: © 2025 by the authors. Licensee MDPI, Basel, Switzerland. This article is an open access article distributed under the terms and conditions of the Creative Commons Attribution (CC BY) license (https://creativecommons.org/licenses/by/4.0/).

1. Introduction

The growing interest in renewable energy as a replacement for fossil fuels is driven by the urgent need to reduce the impact of climate change, environmental pollution and ensure sustainable practices [1]. This shift aligns with several Sustainable Development Goals (SDGs), notably SDG 7 (Affordable and Clean Energy), SDG 13 (Climate Action), and SDG 9 (Industry, Innovation, and Infrastructure) [2]. Renewable energy sources, such as solar, wind, and hydroelectric power, offer clean, inexhaustible alternatives to fossil fuels, which are major contributors to greenhouse gas emissions and environmental degradation [1]. The transition to renewables supports SDG 7 by promoting energy access and security through sustainable energy solutions, contributes to SDG 13 by reducing carbon footprints

and fostering resilience to climate impacts, and stimulates technological innovation and infrastructure development in line with SDG 9, creating jobs and driving economic growth while prioritizing environmental stewardship [2].

Following this changing mindset, catalyzed by current requirements, the growing interest in hydrogen (H_2) energy is driven by its potential to revolutionize the energy sector with its versatility, efficiency, and environmental benefits [3]. As a clean energy carrier, H_2 can be produced from various renewable sources and emits only water vapor when used, making it a key player in the transition to a sustainable clean energy future [3]. Its applications span across multiple fields, including transportation, industry, and power generation, providing a flexible solution for reducing carbon emissions and enhancing energy security [4]. The development of H_2 fuel cells and advancements in H_2 storage and distribution technologies are accelerating the adoption of H_2 energy, supported by significant investments and favorable policies worldwide [4]. As countries and companies intensify their commitments to sustainable energy, H_2 is poised to play a critical role in reshaping the global energy landscape [3].

Palladium (Pd)-based membrane composites are vital in industrial applications, particularly for H_2 purification and separation, due to their exceptional permeability and selectivity [5]. These membranes are constructed by incorporating Pd into various supports like ceramics, metals, and polymers, and these membranes benefit from the mechanical strength and enhanced performance provided by the supports [6]. Techniques such as electroless plating, chemical vapor deposition, and physical vapor deposition are used to deposit Pd onto porous supports, influencing the membrane's durability and efficiency [7]. Palladium's high H_2 permeability and selectivity arise from its ability to allow only hydrogen atoms to diffuse through its lattice, with thinner Pd layers generally providing better performance, albeit with increased susceptibility to defects such as pinholes or micro-cracks [3,5]. The mechanical and thermal stability of these composites is critical for industrial applications. This stability is often enhanced by combining Pd with robust materials, which proves especially critical in high-temperature environments where ceramic supports are advantageous [8]. Operationally, H_2 flux serves as a key performance feature, influenced by factors like membrane thickness, temperature, and pressure difference, with higher temperatures typically increasing flux but also requiring materials that can withstand thermal stress [9]. Durability and longevity are enhanced through strategies like developing Pd alloys and incorporating protective coatings, with Pd-Ag alloys offering improved mechanical properties and resistance to embrittlement [10]. Fouling and contamination present significant operational challenges and can be mitigated through surface modifications and the pre-treatment of feed gas [11]. These composites are used extensively in H_2 purification, fuel cells, chemical industries, and ammonia production, reflecting their importance in achieving high-purity H_2 and efficient separation processes [5,8,12].

Ongoing research aims to further improve the performance and durability of Pd-based membranes, facilitating their broader adoption in H_2-related technologies. Additionally, the application of machine learning techniques in membrane science is revolutionizing the understanding and optimization of materials [13–16]. Principal Component Analysis (PCA), in particular, is valuable for elucidating the physical and chemical properties and operational features of membranes [13–16]. By reducing the dimensionality of complex datasets, PCA identifies the most significant variables affecting membrane performance, enabling more efficient design and predictive maintenance [15,16]. This analytical approach helps experimentalists pinpoint key factors such as material composition, structural characteristics, and operational conditions, leading to improved membrane functionality and longer lifespans [13–16]. The integration of PCA with membrane technology not

only enhances current capabilities but also accelerates the development of next-generation membranes with superior performance and reliability [13].

PCA excels in dimensionality reduction, simplifying datasets with multiple interdependent variables into a smaller set of principal components (PCs) while retaining most of the variance. It effectively identifies hidden patterns and variable interdependencies, offering insights often missed through traditional parametric analysis [13–16]. Additionally, PCA provides clear graphical outputs, such as biplots, enabling the easy visualization of relationships, clustering, and variable contributions. Unlike methods requiring predefined assumptions, PCA is a flexible, data-driven approach suitable for exploratory analysis. For instance, Partial Least Squares Regression (PLSR) focuses on predictive modeling and covariance between input and output variables, making it more suitable with defined dependent variables [13–16]. Factor Analysis (FA), by contrast, assumes underlying latent variable structures, diverging from PCA's purely variance-driven methodology. Hierarchical Cluster Analysis (HCA) focuses on grouping data based on similarity but lacks PCA's dimensionality reduction capability. Similarly, Multiple Linear Regression (MLR) excels in identifying causal relationships but struggles with multicollinearity and hidden variable dependencies, areas where PCA outperforms. In summary, PCA is an unparalleled tool for unbiased exploratory analysis, highlighting key variable contributions and offering insights critical for optimizing Pd-based membrane composites [13–16].

This study aims to evaluate the potential of PCA as a tool for understanding the physical and operational characteristics of Pd-based membrane composites. By examining data from the prior study conducted by Basile et al. [3] (Table 1), this study seeks to uncover hidden relationships among variables such as temperature, differential pressure, thickness, hydrogen permeability, and flux. PCA, an unsupervised machine learning technique, simplifies complex data by reducing its dimensionality, allowing patterns to emerge, correlations to be identified, and the significance of PCs to be assessed within the dataset. These findings are aligned with established knowledge and showcase PCA's ability to highlight meaningful connections providing researchers with clearer insights into the factors influencing membrane performance. This analysis, which focuses on five key variables across 29 membranes, demonstrates PCA's potential to optimize experimental designs, refine manufacturing techniques, and enhance the application of specific Pd-based composites. Unlike traditional studies that focus on isolated variables, our PCA-driven approach reveals deeper interdependencies among membrane characteristics, offering a robust framework for optimizing membrane design and enhancing industrial application feasibility. By revealing hidden trends and uncovering valuable insights, PCA proves to be a powerful statistical tool for advancing our understanding and improving the efficiency of hydrogen production technologies.

This study advances hydrogen separation technology by using PCA to optimize Pd-based membrane composites. The approach identifies key interdependencies among operational parameters and explores sustainable material alternatives, such as chitosan-based membranes. These insights are crucial for refining experimental designs, improving membrane efficiency, and accelerating the adoption of eco-friendly hydrogen separation technologies.

2. Materials and Methods

2.1. Data Normalization and PCA

The data for each investigated variable carry a different weight. To calibrate the influence of these variables on the dataset, a standardization technique is necessary. This method is defined as 'Y_{st}'. It is identified as follows:

$$Y_{st} = \frac{Value - Mean}{Standard\ Deviation} \quad (1)$$

2.2. PCA

After normalization, PCA findings were obtained using XLSTAT 2024.3.0 software (Addinsoft, Paris, France), following the approach in previous studies [13–15,17,18]. In this study, missing data were estimated using a built-in feature that replaces missing values with the "Mode", corresponding to the respective variable.

The jth PC matrix (F_i) is expressed using a unit-weighting vector (U_j) and the original data matrix M with m × n dimensions (m: number of variables, n: number of datasets) as follows [13–15,17,18]:

$$Fi = U_j^T M = \sum^{i=0} U_{ji} M_i \quad (2)$$

where U is the loading coefficient, and M is the data vector of size n. The variance matrix *M(Var(M))* was obtained by projecting M to U, which was maximized, as the following:

$$Var(M) = \frac{1}{n}(UM)(UM)^T = \frac{1}{n}UMM^TU \quad (3)$$

$$MaxVar(M) = Max\left(\left(\frac{1}{n}\right)UMM^TU\right) \quad (4)$$

Since $\frac{1}{n}MM^T$ is the same as the covariance matrix of *M(cov(M))*, *Var(M)* can be expressed as the following:

$$Var\ (M) = U^T cov\ (M)\ U \quad (5)$$

The Lagrangian function can be defined by performing the Lagrange multiplier method, as follows:

$$L = U^T \quad (6)$$

$$L = U^T cov(M)U - \delta\left(U^TU - 1\right) \quad (7)$$

For (7), "U^TU-1" is considered to be equal to zero, since the weighting vector is a unit vector. Hence, the maximum value of var(M) can be calculated by equating the derivative of the Lagrangian function (L), in respect to U, as follows:

$$\frac{dL}{dU} = 0 \quad (8)$$

$$cov(M)\mathrm{U} - \delta U = (cov(M) - \delta I)U = 0 \quad (9)$$

where

δ: eigenvalue of *cov(M)*;

U: eigenvector of *cov(M)*.

To enhance the explanatory power of PCA, two data segmentation schemes were employed: (1) an outlier exclusion scheme aimed at reducing data skewness by removing disproportionately influential samples, and (2) a subset partitioning scheme based on positive and negative correlations of data points along PC1 and PC2. These approaches improved the clarity of clustering patterns and increased the total variance explained across subsets.

Table 1. Physical and operational properties of Pd-based membrane composite [3].

Membrane Type	#	T [K]	ΔP (kPa)	Thickness [μm]	FluxH_2 (mol/m^{2}s)	PeH_2 (mol/m^{2}s Pa)	References
Pd–ZrO_2–PSS [a]	1	773	100	10	0.083	0.0083	[19]
Pd–αAl_2O_3	2	573	290	1	2.05	0.0038	[20]
Pd–Al_2O_3	3	723		4.8		0.000003	[21]
Pd/Ag–Al_2O_3	4		142	10	0.142	0.000001	[22]
Pd/Ag–PSS	5	723	1000	29			[23]
Pd–PSS	6	683		20			[24]
Pd–Al_2O_3	7	573	30	3	0.15	0.000006	[25]
Pd–GCM [b]	8	473	10	15	0.223	0.00000223	[26]
Pd–Al_2O_3	9	801		2.5		0.00000162	[27]
Pd/Ag–PSS	10	723	162	50			[28]
Melt-spun Zr–Al–Co–Ni–Cu	11	673	390	44	0.0044	1.13×10^{-8}	[29]
Pd alloy/PNS [c]	12	773	358		0.083		[30]
Pd–Cu alloy	13	725		0.75	1.6		[31]
Pd/Ni	14	673	20	2.5	0.31	0.0000115	[32]
Pd/Ag alloy	15	620	400	5.5		0.000001	[33]
Pd/MPSS [d]	16	773	100	6	0.302	0.00000302	[34]
Pd	17	473	51	95	0.0267	5.235×10^{-7}	[19]
Pd84–Cu16/ ZrO_2–PSS	18	753	250	5	0.6	0.0005265	[35]
Pd/PSS	19	773	100	11.7		0.000791	[36]
Pd90–Ag10–α Al_2O_3	20	544.5	165	20	0.14	0.00000125	[37]
Pd–CS [e]	21	698	400	2		0.000001688	[38]
Pd/Pd–Ag–PSS	22	723	100	2.5	0.3	0.000003	[34]
Pd–Ag/αFe_2O_3/ PSS	23	773	300	18		0.000491	[39]
Pd–Cu/αAl_2O_3	24	723	345	11	0.8	0.00000231	[40]
Pd/TiO_2	25	773	45	0.35	0.283	0.00000628	[41]
Pd–Ni/SS	26	723	68	0.8	0.7265	0.00001051	[42]
Pd–Ru–In/SS	27	645	100	1.5	0.049	0.00000049	[43]
Pd–Al_2O_3	28	673	100	5	0.155	0.00000155	[44]
Pd/PSS	29	793	150	10	0.175	0.000001166	[45]

[a] PSS: polystyrene sulfonate; [b] GCM: graphene composite membrane; [c] PNS: porous nickel support; [d] MPSS: macro-porous stainless steel; and [e] CS: chitosan.

3. Results and Discussion

This study employs PCA to examine differences and similarities among a group of Pd-based membrane composites by analyzing five key physical and operational factors: temperature, differential pressure (ΔP), thickness, H_2 permeability, and H_2 flux. It is anticipated that the first two PCs will account for a significant portion of the total variance, shedding light on the relationships among these variables. To enhance the explanatory power of the PCs and validate observed trends, two data segmentation strategies are proposed. The first involves removing outliers identified via the PCA biplot. The second strategy entails dividing the dataset into four subsets based on the positive and negative correlations of the first two PCs. These data-driven approaches, guided solely by PCA outcomes rather than preconceived engineering assumptions, are expected to refine comparisons among membranes and uncover deeper insights into the variables affecting their performance.

3.1. PCA for the Entire Dataset

Figure 1 shows that the PCA presentation of the dataset for Pd-based composite membranes has been taken into consideration (data originate from the investigations of Basile et al. [3]). The first two PCs accounted for 53.16% of the total variance, with PC1 and PC2 contributing 31.49% and 21.68%, respectively; Figure 1a). This level of variance is moderate compared to previous investigations applying PCA to membrane

datasets [13–15,17,18]. The investigated variables showed moderate contributions along PC_1 (between 20 and 40%; Figure 1b), except for PeH2 and ΔP, which showed low and minor contributions, respectively (Figure 1b). For PC_2, most of its contribution accounted for ΔP (67.81; Figure 1b), with a minor and negligible contributions for the other variables. PCA generates new orthogonal variables (PCs) by eliminating intercorrelations between the input variables. The observed indicate interdependencies among the variables, except for ΔP. In other words, ΔP is found to be independent from the other variables, for the Pd-based membranes under study. Hence, optimizing Pd-based membranes requires a synergetic consideration of temperature, thickness, and $FluxH_2$, with lesser emphasis of PeH_2. On the other hand, ΔP should be considered as an independent variable.

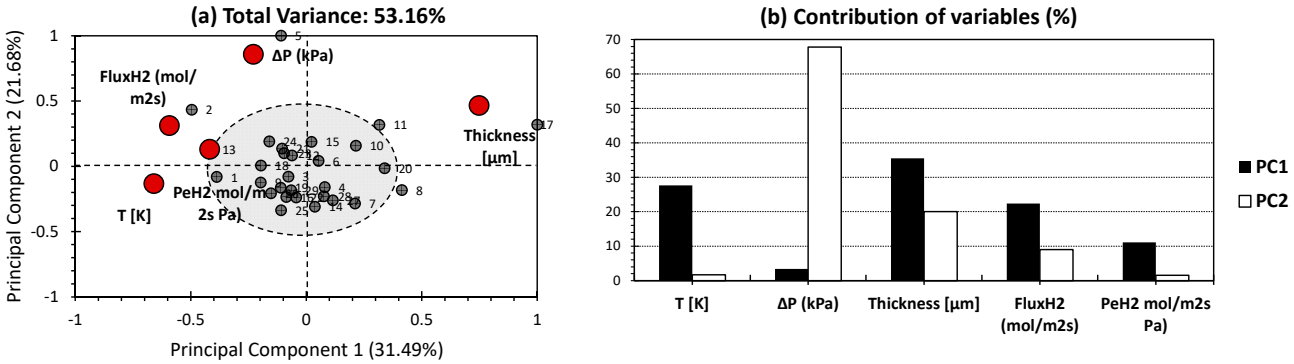


Figure 1. PCA biplot for all datasets (data originate from the investigations of Basile et al. [3]). Gray bullets highlight the individuals of the population (different investigated Pd-based composite membranes). Red bullets represent the variables (adopted physical properties and operational conditions).

When considering all membranes (the individuals of the statistical analysis), a significant agglomeration around the node can be observed (gray cluster; Figure 1a). The highest loadings are noted for membranes 2, 5, and 17. These trends suggest several scenarios: (a) Most of the investigated membranes exhibit a similar behavior toward the investigated physical and operational conditions explored, discarding the difference between membranes at the molecular composition's level. (b) The investigated variables have a minor influence on the membranes in-hand. (c) The individuals with the highest loadings (membranes 2, 5, and 17) have skewed the dispersion of clustered samples around the node. To confirm or refute any of the three addressed possibilities, data partitioning could be adopted, following the yielded trends in Figure 1. Hence, a PCA was performed for this dataset, with the exclusion of the different outliers (membranes 2, 5, and 17) (Figure 2). Another strategy could involve dividing the dataset into four subsets without relying on engineering or scientific intuition for decision making. The division is purely statistical, following the observed trends in the overall dataset (Figure 1). Four PCAs could be performed based on the positive and/or negative trends of samples, following the first two PCs (Figures 3–6).

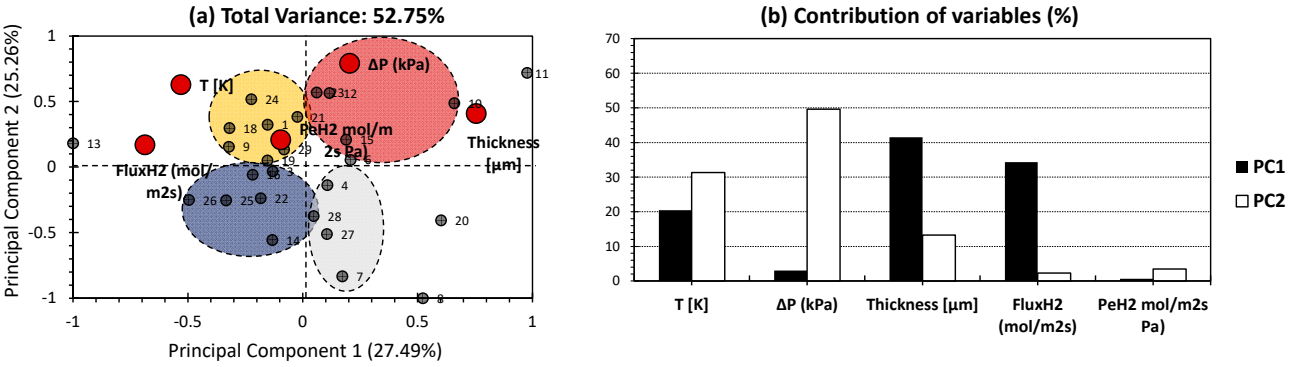


Figure 2. PCA biplot for all datasets (data originate from the investigations of Basile et al. [3]), with the exclusion of outliers in Figure 1 (Membranes 2, 5, and 17). Gray bullets highlight the individuals of the population (different investigated Pd-based composite membranes). Red bullets represent the variables (adopted physical properties and operational conditions).

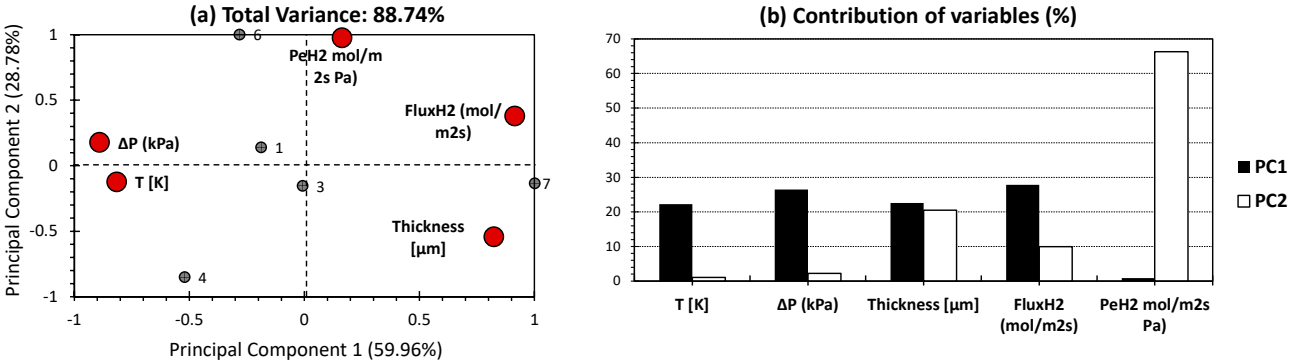


Figure 3. PCA biplot for the dataset positively correlated along the two PCs of Figure 1 (data originate from the investigations of Basile et al. [3]). Gray bullets highlight the individuals of the population (different investigated Pd-based composite membranes). Red bullets represent the variables (adopted physical properties and operational conditions).

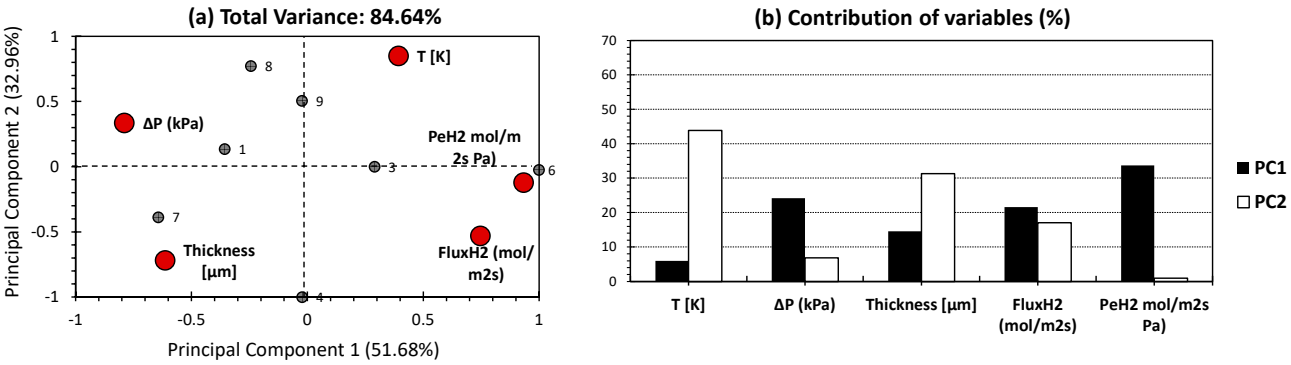


Figure 4. PCA biplot for the dataset positively correlated along PC_1, and negatively correlated along PC_2 of Figure 1 (data originate from the investigations of Basile et al. [3]). Gray bullets highlight the individuals of the population (different investigated Pd-based composite membranes). Red bullets represent the variables (adopted physical properties and operational conditions).

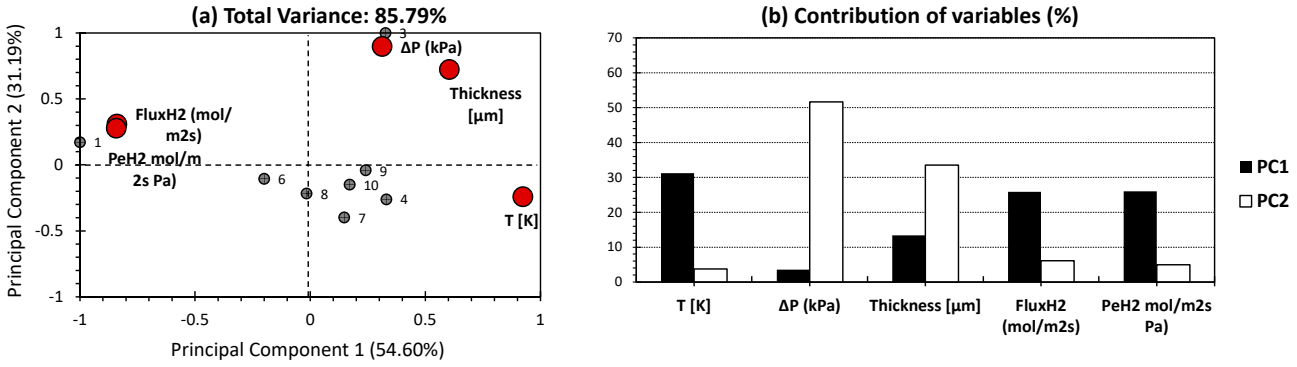


Figure 5. PCA biplot for the dataset negatively correlated along PC_1 and positively correlated along PC_2 of Figure 1 (data originate from the investigations of Basile et al. [3]). Gray bullets highlight the individuals of the population (different investigated Pd-based composite membranes). Red bullets represent the variables (adopted physical properties and operational conditions).

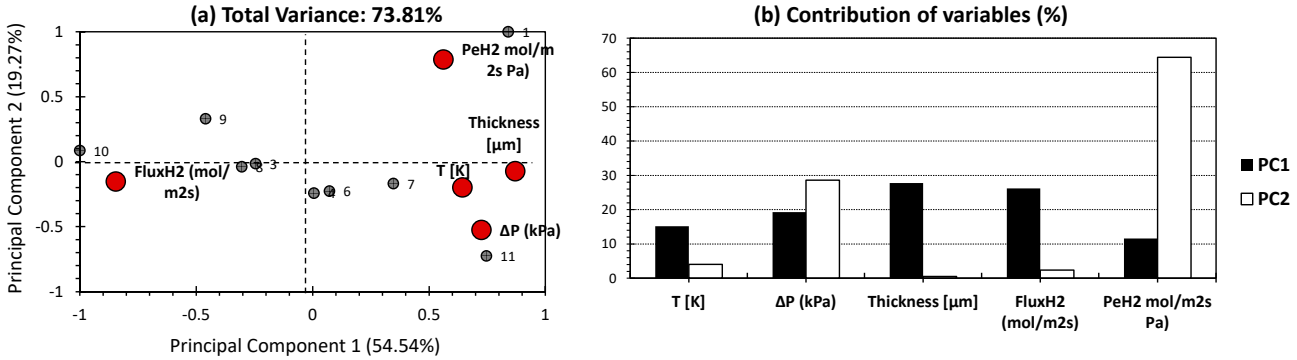


Figure 6. PCA biplot for the dataset negatively correlated along the two PCs of Figure 1 (data originate from the investigations of Basile et al. [3]). Gray bullets highlight the individuals of the population (different investigated Pd-based composite membranes). Red bullets represent the variables (adopted physical properties and operational conditions).

3.2. PCA with the Exclusion of Outliers

Figure 2 shows the PCA presentation with the exclusion of outliers (membranes 2, 5, and 17). The first two PCs accounted for a presentation nearly similar to the entire dataset approach (52.75% of total variance, 27.49% for PC_1, and 25.26% for PC_2; Figure 2b). This high similarity would indicate that scenario (a) is more likely plausible than scenario (c) (See Section 3.1.). It is worth mentioning that discarding the outliers allowed for the better separation of different samples and led to the formation of four different clusters (Figure 2). For the variables, a noticeable separation can be identified among the variables, except for temperature. In other words, the variable that exhibited moderate/high contribution around PC_1 did not manifest any distinct contribution along PC_2 and vice versa. The highest contributions were scored for thickness and $FluxH_2$ (41.51% and 34.30%, respectively; Figure 2b), along with PC_1. A moderate contribution were scored for Temperature (20.48%; Figure 2b). For ΔP and PeH_2, they showed minor contributions along PC_1. For PC_2, most of the contribution was distributed between T and ΔP, scoring 31.33% and 49.66%, respectively (Figure 2b). The rest of the variables exhibited low to minor contributions for PC_2. These trends highlight the high dependency between the adopted temperature and thickness, permeability, and hydrogen flux, which should be considered when employing Pd-based composite membranes. This relationship was obscured in the full dataset approach.

The analysis identified four distinct clusters for the individuals, corresponding to the four parts of the PCA biplot (Figure 2a). This indicates the relevance of splitting the data into the four corresponding subsets (Figures 4–6). The red cluster was plotted on the positive

sides of both PCs, indicating a positive correlation between the variables represented by ΔP and PC_2. This cluster contained membranes 6, 12, 15, and 23. In fact, several studies investigated Pd–PSS and identified its benefits in offering good performance under high pressure due to the strength of polysulfone support and benefits from a thin Pd layer for high permeability [5,8,10]. For the Pd alloy/PNS, it provides excellent high-pressure resistance and high permeability, with the porous nanosilica support offering additional stability and surface area [30]. The Pd/Ag alloy exhibits the capacity to synergistically work in high-pressure durability and very high H_2 flux, due to the beneficial properties of the Pd-silver alloy [5,46]. Following its polysulfone support, Pd–Ag/αFe_2O_3/PSS balances high-pressure performance and thin membrane benefits through a composite structure, enhancing both mechanical stability and H_2 permeability [3].

For the yellow cluster, it was plotted on the negative and positive sides of PC_1 and PC_2, respectively, and exhibited a positive correlation with temperature and permeability towards H_2. For the Pd–ZrO_2–PSS composite, the integration of ZrO_2 enhances mechanical stability, ensuring that the membrane maintains its integrity under high temperatures [9]. Sanz et al. [47] revealed higher H_2 fluxes with the increase in temperature, indicating improved performance with this type of membrane. These findings are in total accordance with the PCA trends, as temperature and H_2 flux both exhibited a negative effect along PC_1 and a positive effect along PC_2 (Figure 2a). In terms of durability, PSS substrate provides structural support, making the membrane robust against physical stresses and long-term use in harsh environments [12]. In addition, ZrO_2 imparts chemical resistance when exposed to high temperatures, protecting the membrane from degradation by contaminants [11,48]. For the Pd–Al_2O_3 composite, the thermal stability of Al_2O_3 offers excellent resistance, allowing the membrane to operate effectively at high temperatures [49]. In addition, related membrane composites exhibit good thermal stability (up to ~550 °C [50]), allowing their applications under high operating temperature conditions [6]. In terms of enhanced durability, Al_2O_3 contributes to the membrane's resistance to chemical attack, extending its operational lifespan [51,52]. In addition, this composite's structure combines the strengths of both materials (Pd and Al_2O_3), resulting in a membrane that performs well under demanding conditions [53,54]. For the Pd84–Cu16/ZrO_2–PSS composite, the Pd–Cu alloy improves H_2 permeability and selectivity, yielding an efficient trade-off between performance and cost [55,56]. In terms of thermal resilience, the implementation of ZrO_2 in such composites enhances resistance to degradation, while PSS provides a robust support [52]. On the other hand, the addition of copper reduces palladium's susceptibility to H_2 embrittlement, increasing the membrane's durability [57]. In terms of mechanical properties, this composite is designed to withstand high pressure and temperature, making it ideal for industrial applications [58]. For the Pd–CS composite, chitosan (CS) offers a sustainable and potentially lower-cost alternative to synthetic materials [59]. It enhances the membrane's flexibility and structural integrity, supporting the Pd layer [60]. Pd maintains high H_2 permeability and selectivity, ensuring efficient separation [61]. In addition, the natural origin of chitosan adds an element of biocompatibility, making the membrane more environmentally friendly [62]. The findings of PCA show that this Pd-based membrane could be an eco-friendly substitute for the other six membranes of the same cluster (Figure 2a). The Pd–Cu/αAl_2O_3 composite combines the enhanced permeability and selectivity from the Pd–Cu [55,56] with the thermal and mechanical strength of Al_2O_3 [53,54]. This coupling ensures that the membrane can operate efficiently under high-temperature and high-pressure conditions, making it ideal for demanding industrial processes [55,56].

3.3. PCA of Subsets

For the sake of increasing PCA's efficiency toward revealing hidden patterns in the Pd-based membrane composite, this analysis was performed on four subsets, following the positive/negative trends of the PCA of the whole dataset (Figure 1). This approach increased the total variance to at least 73% (Figure 6). When exclusively considering the membrane samples with positive scores on both principal components in Figure 1, the PCA biplot showed 88.74% of the total variance (59.96% and 28.78% for PC_1 and PC_2, respectively; Figure 3a).

The high variance would indicate the higher rate of presentation for the PCA when subsets are acquired [13–15,17,18]. This would increase the reliability of PCA findings. For the variables, all physical and operational features, apart from PeH_2, have shown moderate contribution along PC_1 (around 20–30%; Figure 3b). For the latter, it encompassed most of the contribution along PC_2 (scoring 66.26%; Figure 3b). The rest of the variables exhibited minor to negligible influence for this PC. This would indicate that permeability towards H_2 for the investigated membranes (1, 3, 4, 6, and 7) is more likely independent of the other four variables at hand. Figure 4 shows the PCA investigation for membrane samples that showed a positive correlation along PC1 and a negative one along PC2, when the entire dataset was considered (Figure 1). The PCA biplot showed a total variance of 84.64% (51.68% and 32.96% along PC_1 and PC_2, respectively; Figure 4a). For the variables, the highest contribution was yielded for PeH_2, accounting for 33.70% of PC_1 (Figure 4b). Except for temperature, the rest of the variables showed minor to moderate contribution (from 14% to 24%; Figure 4b). For PC_2, the highest contribution was scored for temperature, accounting for 43.84% (Figure 4b). For FluxH2 and thickness, minor and moderate contributions occurred (17.06% and 31.32%, respectively; Figure 4b). Figure 5 shows the PCA investigation for membrane samples that showed a negative correlation along PC1 and a positive one along PC2 when the entire dataset was considered. The PCA biplot showed a total variance of 85.79% (54.60% and 31.19% along PC_1 and PC_2, respectively; Figure 5a). For the variables, moderate contributions were yielded for PeH_2, $FluxH_2$, and temperature (from 25% to 30%; Figure 5b). For PC2, the highest contribution was yielded for ΔP and thickness, accounting for 51.66% and 33.53%, respectively (Figure 5b). This shows a good independency between the variables mostly yielded along both PCs. An even higher discrepancy between variables was noticed for the negatively yielded samples on the first two PCs, when the entire dataset was taken into consideration. These trends are shown in the PCA biplot of Figure 6. In fact, all variables have shown low to moderate contribution along PC1 (Figure 6b), while PC2 was mostly dominated by PeH2 (64.39%; Figure 6b). In brief, the discrepancies between trends in PCA subsets are primarily influenced by the type of samples included in the analysis. Each subset showed reliance on several sets of variables. In addition, the increase in total variance confirms the necessity of data splitting to achieve a better comparison between the different samples.

4. Conclusions

This study applied the so-called Principal Component Analysis (PCA) technique for revealing discrepancies and similarities between a set of Pd-based membrane composites, following five physical and operational features: temperature, differential pressure, thickness, H_2 permeability, and H_2 flux. When the entire dataset was considered, the first two principal components (PCs) accounted for 53.16% of the total variance. This contribution was found to be moderate, in comparison with previous investigations of the application of PCA for the membranes' datasets. The different trends would indicate an interdependency existing between all variables at hand, except for ΔP. Hence, an optimization of Pd-based membranes implies the requirement to consider a synergetic interplay between

temperature, thickness, $FluxH_2$, and PeH_2, on one hand. On the other hand, ΔP should be considered independently.

For the sake of attempting to increase total variance and to confirm or refute a valid comparison between the investigated membranes, two strategies of data separation were adopted. Both strategies were followed without any engineering intuition and only accounted for the trends of the PCA biplot for the entire dataset. The first strategy involves excluding the outliers of the PCA for the entire dataset: membranes 2, 5, and 17, in our case. The second one states the partitioning of the dataset into four subsets based on the negative/positive trends of the first two PCs.

For the PCA approach without outliers, it showed a similar variance as the first approach. This would indicate that most of the investigated membranes exhibit a similar behavior under the investigated physical and operational conditions explored. It is worth mentioning that discarding the outliers allowed more distribution of different samples and led to the formation of four different clusters, hence allowing certain distinctions between membranes. PCA without outliers allowed the revelation of high dependency between the adopted temperature and the differential pressure. This accordance was hidden from the whole dataset approach. The yielded clustering of PCA showed a high similarity between sets of Pd-based membranes, including a chitosan based one. The latter could be an eco-friendly substitute for the other six membranes of the same cluster: Pd–PSS, Pd alloy/PNS, Pd–ZrO_2–PSS, Pd–Al_2O_3, Pd84–Cu16/ZrO_2–PSS, and Pd–Cu/αAl_2O_3.

For the sake of increasing PCA's efficiency toward revealing hidden patterns, data separation into subsets was adopted. This strategy raised the total variance from 73% to 86%. The discrepancies between trends of PCA in subsets are mostly explained by the type of samples included in the analysis. Each subset showed a reliance on several sets of variables. Hence, the PCA approach can be used for in situ experimentation to optimize the experimental procedure.

Author Contributions: Conceptualization, K.Y.; Methodology, K.Y.; Software, K.Y.; Validation, M.H.; Investigation, W.A.-S.; Data curation, K.Y. and C.E.S.; Writing—original draft, K.Y., W.A.-S., M.H., M.F. and C.E.S.; Writing—review & editing, W.A.-S., M.H., M.F., S.B. and C.E.S.; Visualization, W.A.-S.; Project administration, K.Y. and C.E.S. All authors have read and agreed to the published version of the manuscript.

Funding: This research received no external funding.

Data Availability Statement: The data presented and treated in this study are available from "Synthesis, Characterization, and Applications of Palladium Membranes" [https://doi.org/10.1016/S0927-5193(07)13008-4].

Conflicts of Interest: There are no conflicts of interest to declare.

References

1. Zhang, J. Energy Access Challenge and the Role of Fossil Fuels in Meeting Electricity Demand: Promoting Renewable Energy Capacity for Sustainable Development. *Geosci. Front.* **2024**, *15*, 101873. [CrossRef]
2. Abbasi, K.R.; Zhang, Q.; Alotaibi, B.S.; Abuhussain, M.A.; Alvarado, R. Toward Sustainable Development Goals 7 and 13: A Comprehensive Policy Framework to Combat Climate Change. *Environ. Impact Assess. Rev.* **2024**, *105*, 107415. [CrossRef]
3. Basile, A.; Gallucci, F.; Tosti, S. Synthesis, Characterization, and Applications of Palladium Membranes. *Membr. Sci. Technol.* **2008**, *13*, 255–323.
4. Gritz, A.; Wolff, G. Gas and Energy Security in Germany and Central and Eastern Europe. *Energy Policy* **2024**, *184*, 113885. [CrossRef]
5. Al-Mufachi, N.A.; Rees, N.V.; Steinberger-Wilkens, R. Hydrogen Selective Membranes: A Review of Palladium-Based Dense Metal Membranes. *Renew. Sustain. Energy Rev.* **2015**, *47*, 540–551. [CrossRef]

6. Rothenberger, K.S.; Cugini, A.V.; Howard, B.H.; Killmeyer, R.P.; Ciocco, M.V.; Morreale, B.D.; Enick, R.M.; Bustamante, F.; Mardilovich, I.P.; Ma, Y.H. High Pressure Hydrogen Permeance of Porous Stainless Steel Coated with a Thin Palladium Film via Electroless Plating. *J. Membr. Sci.* **2004**, *244*, 55–68. [CrossRef]
7. Al-Shaeli, M.; Teber, O.O.; Al-Juboori, R.A.; Khataee, A.; Koyuncu, I.; Vatanpour, V. Inorganic Layered Polymeric Membranes: Highly-Ordered Porous Ceramics for Surface Engineering of Polymeric Membranes. *Sep. Purif. Technol.* **2024**, 127925. [CrossRef]
8. Gallucci, F.; Fernandez, E.; Corengia, P.; van Sint Annaland, M. Recent Advances on Membranes and Membrane Reactors for Hydrogen Production. *Chem. Eng. Sci.* **2013**, *92*, 40–66. [CrossRef]
9. Zhang, K.; Gao, H.; Rui, Z.; Liu, P.; Li, Y.; Lin, Y.S. High-Temperature Stability of Palladium Membranes on Porous Metal Supports with Different Intermediate Layers. *Ind. Eng. Chem. Res.* **2009**, *48*, 1880–1886. [CrossRef]
10. Pal, N.; Agarwal, M.; Maheshwari, K.; Solanki, Y.S. A Review on Types, Fabrication and Support Material of Hydrogen Separation Membrane. *Mater. Today: Proc.* **2020**, *28*, 1386–1391. [CrossRef]
11. Chen, C.; Lu, L.; Fei, L.; Xu, J.; Wang, B.; Li, B.; Shen, L.; Lin, H. Membrane-Catalysis Integrated System for Contaminants Degradation and Membrane Fouling Mitigation: A Review. *Sci. Total Environ.* **2023**, *904*, 166220. [CrossRef] [PubMed]
12. Arratibel Plazaola, A.; Pacheco Tanaka, D.A.; Van Sint Annaland, M.; Gallucci, F. Recent Advances in Pd-Based Membranes for Membrane Reactors. *Molecules* **2017**, *22*, 51. [CrossRef] [PubMed]
13. Murshid, N.; Mouhtady, O.; Abu-Samha, M.; Obeid, E.; Kharboutly, Y.; Chaouk, H.; Halwani, J.; Younes, K. Metal Oxide Hydrogel Composites for Remediation of Dye-Contaminated Wastewater: Principal Component Analysis. *Gels* **2022**, *8*, 702. [CrossRef] [PubMed]
14. Younes, K.; Kharboutly, Y.; Antar, M.; Chaouk, H.; Obeid, E.; Mouhtady, O.; Abu-samha, M.; Halwani, J.; Murshid, N. Application of Unsupervised Machine Learning for the Evaluation of Aerogels' Efficiency towards Ion Removal—A Principal Component Analysis (PCA) Approach. *Gels* **2023**, *9*, 304. [CrossRef] [PubMed]
15. Mouhtady, O.; Obeid, E.; Abu-samha, M.; Younes, K.; Murshid, N. Evaluation of the Adsorption Efficiency of Graphene Oxide Hydrogels in Wastewater Dye Removal: Application of Principal Component Analysis. *Gels* **2022**, *8*, 447. [CrossRef]
16. Peiris, R.H.; Budman, H.; Moresoli, C.; Legge, R.L. Development of a Species Specific Fouling Index Using Principal Component Analysis of Fluorescence Excitation–Emission Matrices for the Ultrafiltration of Natural Water and Drinking Water Production. *J. Membr. Sci.* **2011**, *378*, 257–264. [CrossRef]
17. Younes, K.; Mouhtady, O.; Chaouk, H.; Obeid, E.; Roufayel, R.; Moghrabi, A.; Murshid, N. The Application of Principal Component Analysis (PCA) for the Optimization of the Conditions of Fabrication of Electrospun Nanofibrous Membrane for Desalination and Ion Removal. *Membranes* **2021**, *11*, 979. [CrossRef]
18. Younes, K.; Moghnie, S.; Khader, L.; Obeid, E.; Mouhtady, O.; Grasset, L.; Murshid, N. Application of Unsupervised Learning for the Evaluation of Burial Behavior of Geomaterials in Peatlands: Case of Lignin Moieties Yielded by Alkaline Oxidative Cleavage. *Polymers* **2023**, *15*, 1200. [CrossRef]
19. Wang, D.; Tong, J.; Xu, H.; Matsumura, Y. Preparation of Palladium Membrane over Porous Stainless Steel Tube Modified with Zirconium Oxide. *Catal. Today* **2004**, *93*, 689–693. [CrossRef]
20. Sato, K.; Hanaoka, T.; Niwa, S.; Stefan, C.; Namba, T.; Mizukami, F. Direct Hydroxylation of Aromatic Compounds by a Palladium Membrane Reactor. *Catal. Today* **2005**, *104*, 260–266. [CrossRef]
21. Van Dyk, L.; Miachon, S.; Lorenzen, L.; Torres, M.; Fiaty, K.; Dalmon, J.-A. Comparison of Microporous MFI and Dense Pd Membrane Performances in an Extractor-Type CMR. *Catal. Today* **2003**, *82*, 167–177. [CrossRef]
22. Liang, W.; Hughes, R. The Catalytic Dehydrogenation of Isobutane to Isobutene in a Palladium/Silver Composite Membrane Reactor. *Catal. Today* **2005**, *104*, 238–243. [CrossRef]
23. Lin, W.-H.; Chang, H.-F. A Study of Ethanol Dehydrogenation Reaction in a Palladium Membrane Reactor. *Catal. Today* **2004**, *97*, 181–188. [CrossRef]
24. Lin, Y.-M.; Liu, S.-L.; Chuang, C.-H.; Chu, Y.-T. Effect of Incipient Removal of Hydrogen through Palladium Membrane on the Conversion of Methane Steam Reforming: Experimental and Modeling. *Catal. Today* **2003**, *82*, 127–139. [CrossRef]
25. Itoh, N.; Akiha, T.; Sato, T. Preparation of Thin Palladium Composite Membrane Tube by a CVD Technique and Its Hydrogen Permselectivity. *Catal. Today* **2005**, *104*, 231–237. [CrossRef]
26. Altinisik, O.; Dogan, M.; Dogu, G. Preparation and Characterization of Palladium-Plated Porous Glass for Hydrogen Enrichment. *Catal. Today* **2005**, *105*, 641–646. [CrossRef]
27. Kleinert, A.; Grubert, G.; Pan, X.; Hamel, C.; Seidel-Morgenstern, A.; Caro, J. Compatibility of Hydrogen Transfer via Pd-Membranes with the Rates of Heterogeneously Catalysed Steam Reforming. *Catal. Today* **2005**, *104*, 267–273. [CrossRef]
28. Basile, A.; Gallucci, F.; Paturzo, L. Hydrogen Production from Methanol by Oxidative Steam Reforming Carried out in a Membrane Reactor. *Catal. Today* **2005**, *104*, 251–259. [CrossRef]
29. Shimpo, Y.; Yamaura, S.; Okouchi, H.; Nishida, M.; Kajita, O.; Kimura, H.; Inoue, A. Hydrogen Permeation Characteristics of Melt-Spun Zr60Al15Co2. 5Ni7. 5Cu15 Glassy Alloy Membrane. *J. Alloys Compd.* **2004**, *372*, 197–200. [CrossRef]

30. Ryi, S.-K.; Park, J.-S.; Kim, S.-H.; Cho, S.-H.; Park, J.-S.; Kim, D.-W. Development of a New Porous Metal Support of Metallic Dense Membrane for Hydrogen Separation. *J. Membr. Sci.* **2006**, *279*, 439–445. [CrossRef]
31. Hoang, H.T.; Tong, H.D.; Gielens, F.C.; Jansen, H.V.; Elwenspoek, M.C. Fabrication and Characterization of Dual Sputtered Pd–Cu Alloy Films for Hydrogen Separation Membranes. *Mater. Lett.* **2004**, *58*, 525–528. [CrossRef]
32. Zhang, Y.; Gwak, J.; Murakoshi, Y.; Ikehara, T.; Maeda, R.; Nishimura, C. Hydrogen Permeation Characteristics of Thin Pd Membrane Prepared by Microfabrication Technology. *J. Membr. Sci.* **2006**, *277*, 203–209. [CrossRef]
33. Hou, K.; Hughes, R. Preparation of Thin and Highly Stable Pd/Ag Composite Membranes and Simulative Analysis of Transfer Resistance for Hydrogen Separation. *J. Membr. Sci.* **2003**, *214*, 43–55. [CrossRef]
34. Tong, J.; Suda, H.; Haraya, K.; Matsumura, Y. A Novel Method for the Preparation of Thin Dense Pd Membrane on Macroporous Stainless Steel Tube Filter. *J. Membr. Sci.* **2005**, *260*, 10–18. [CrossRef]
35. Gao, H.; Lin, J.Y.; Li, Y.; Zhang, B. Electroless Plating Synthesis, Characterization and Permeation Properties of Pd–Cu Membranes Supported on ZrO2 Modified Porous Stainless Steel. *J. Membr. Sci.* **2005**, *265*, 142–152. [CrossRef]
36. Mardilovich, I.P.; Engwall, E.; Ma, Y.H. Dependence of Hydrogen Flux on the Pore Size and Plating Surface Topology of Asymmetric Pd-Porous Stainless Steel Membranes. *Desalination* **2002**, *144*, 85–89. [CrossRef]
37. Huang, T.-C.; Wei, M.-C.; Chen, H.-I. Preparation of Hydrogen-Permselective Palladium–Silver Alloy Composite Membranes by Electroless Co-Deposition. *Sep. Purif. Technol.* **2003**, *32*, 239–245. [CrossRef]
38. Zhang, J.; Liu, D.; He, M.; Xu, H.; Li, W. Experimental and Simulation Studies on Concentration Polarization in H2 Enrichment by Highly Permeable and Selective Pd Membranes. *J. Membr. Sci.* **2006**, *274*, 83–91. [CrossRef]
39. Yepes, D.; Cornaglia, L.M.; Irusta, S.; Lombardo, E.A. Different Oxides Used as Diffusion Barriers in Composite Hydrogen Permeable Membranes. *J. Membr. Sci.* **2006**, *274*, 92–101. [CrossRef]
40. Roa, F.; Way, J.D.; McCormick, R.L.; Paglieri, S.N. Preparation and Characterization of Pd–Cu Composite Membranes for Hydrogen Separation. *Chem. Eng. J.* **2003**, *93*, 11–22. [CrossRef]
41. Wu, L.-Q.; Xu, N.; Shi, J. Preparation of a Palladium Composite Membrane by an Improved Electroless Plating Technique. *Ind. Eng. Chem. Res.* **2000**, *39*, 342–348. [CrossRef]
42. Nam, S.-E.; Lee, S.-H.; Lee, K.-H. Preparation of a Palladium Alloy Composite Membrane Supported in a Porous Stainless Steel by Vacuum Electrodeposition. *J. Membr. Sci.* **1999**, *153*, 163–173. [CrossRef]
43. Yan, S.; Maeda, H.; Kusakabe, K.; Morooka, S. Thin Palladium Membrane Formed in Support Pores by Metal-Organic Chemical Vapor Deposition Method and Application to Hydrogen Separation. *Ind. Eng. Chem. Res.* **1994**, *33*, 616–622. [CrossRef]
44. Dittmeyer, R.; Höllein, V.; Daub, K. Membrane Reactors for Hydrogenation and Dehydrogenation Processes Based on Supported Palladium. *J. Mol. Catal. A: Chem.* **2001**, *173*, 135–184. [CrossRef]
45. Liang, W.; Hughes, R. The Effect of Diffusion Direction on the Permeation Rate of Hydrogen in Palladium Composite Membranes. *Chem. Eng. J.* **2005**, *112*, 81–86. [CrossRef]
46. Conde, J.J.; Maroño, M.; Sánchez-Hervás, J.M. Pd-Based Membranes for Hydrogen Separation: Review of Alloying Elements and Their Influence on Membrane Properties. *Sep. Purif. Rev.* **2017**, *46*, 152–177. [CrossRef]
47. Sanz, R.; Calles, J.A.; Alique, D.; Furones, L. H2 Production via Water Gas Shift in a Composite Pd Membrane Reactor Prepared by the Pore-Plating Method. *Int. J. Hydrog. Energy* **2014**, *39*, 4739–4748. [CrossRef]
48. Rajlaxmi; Gupta, N.; Behere, R.P.; Layek, R.K.; Kuila, B.K. Polymer Nanocomposite Membranes and Their Application for Flow Catalysis and Photocatalytic Degradation of Organic Pollutants. *Mater. Today Chem.* **2021**, *22*, 100600. [CrossRef]
49. Weber, M.; Drobek, M.; Rebière, B.; Charmette, C.; Cartier, J.; Julbe, A.; Bechelany, M. Hydrogen Selective Palladium-Alumina Composite Membranes Prepared by Atomic Layer Deposition. *J. Membr. Sci.* **2020**, *596*, 117701. [CrossRef]
50. de Nooijer, N.; Arratibel Plazaola, A.; Meléndez Rey, J.; Fernandez, E.; Pacheco Tanaka, D.A.; van Sint Annaland, M.; Gallucci, F. Long-Term Stability of Thin-Film Pd-Based Supported Membranes. *Processes* **2019**, *7*, 106. [CrossRef]
51. Zahid, M.; Rashid, A.; Akram, S.; Rehan, Z.A.; Razzaq, W. A Comprehensive Review on Polymeric Nano-Composite Membranes for Water Treatment. *J. Membr. Sci. Technol* **2018**, *8*, 1–20. [CrossRef]
52. Singh, H.; Saxena, P.; Puri, Y.M. The Manufacturing and Applications of the Porous Metal Membranes: A Critical Review. *CIRP J. Manuf. Sci. Technol.* **2021**, *33*, 339–368. [CrossRef]
53. Liguori, S.; Iulianelli, A.; Dalena, F.; Pinacci, P.; Drago, F.; Broglia, M.; Huang, Y.; Basile, A. Performance and Long-Term Stability of Pd/PSS and Pd/Al2O3 Membranes for Hydrogen Separation. *Membranes* **2014**, *4*, 143–162. [CrossRef] [PubMed]
54. Tsai, T.K.; Lu, Y.K.; Fang, J.S.; Chen, G.S. Ultrasound Assistance in the Sensitization and Activation of Porous Al2O3 Supports for Improving the Hydrogen Separation of Pd/Al2O3 Composite Membranes. *Int. J. Hydrog. Energy* **2024**, *55*, 1007–1016. [CrossRef]
55. Habib, M.A.; Harale, A.; Paglieri, S.; Alrashed, F.S.; Al-Sayoud, A.; Rao, M.V.; Nemitallah, M.A.; Hossain, S.; Hussien, M.; Ali, A.; et al. Palladium-Alloy Membrane Reactors for Fuel Reforming and Hydrogen Production: A Review. *Energy Fuels* **2021**, *35*, 5558–5593. [CrossRef]
56. Zhao, L.; Goldbach, A.; Xu, H. Tailoring Palladium Alloy Membranes for Hydrogen Separation from Sulfur Contaminated Gas Streams. *J. Membr. Sci.* **2016**, *507*, 55–62. [CrossRef]

57. Perović, K.; Morović, S.; Jukić, A.; Košutić, K. Alternative to Conventional Solutions in the Development of Membranes and Hydrogen Evolution Electrocatalysts for Application in Proton Exchange Membrane Water Electrolysis: A Review. *Materials* **2023**, *16*, 6319. [CrossRef]
58. Paglieri, S.N.; Way, J.D. INNOVATIONS IN PALLADIUM MEMBRANE RESEARCH. *Sep. Purif. Methods* **2002**, *31*, 1–169. [CrossRef]
59. Akter, M.; Uddin, M.H.; Tania, I.S. Biocomposites Based on Natural Fibers and Polymers: A Review on Properties and Potential Applications. *J. Reinf. Plast. Compos.* **2022**, *41*, 705–742. [CrossRef]
60. Balakrishnan, A.; Mariam Jacob, M.; Dayanandan, N.; Chinthala, M.; Ponnuchamy, M.; Vo, D.-V.N.; Appunni, S.; Selvan Gajendhran, A. Chitosan/Metal Organic Frameworks for Environmental, Energy, and Bio-Medical Applications: A Review. *Mater. Adv.* **2023**, *4*, 5920–5947. [CrossRef]
61. Alique, D.; Martinez-Diaz, D.; Sanz, R.; Calles, J.A. Review of Supported Pd-Based Membranes Preparation by Electroless Plating for Ultra-Pure Hydrogen Production. *Membranes* **2018**, *8*, 5. [CrossRef]
62. Jiménez-Gómez, C.P.; Cecilia, J.A. Chitosan: A Natural Biopolymer with a Wide and Varied Range of Applications. *Molecules* **2020**, *25*, 3981. [CrossRef]

Disclaimer/Publisher's Note: The statements, opinions and data contained in all publications are solely those of the individual author(s) and contributor(s) and not of MDPI and/or the editor(s). MDPI and/or the editor(s) disclaim responsibility for any injury to people or property resulting from any ideas, methods, instructions or products referred to in the content.